

Quasi-harmonic thermoelasticity of palladium, platinum, copper, and gold from first principles

Cristiano Malica¹ and Andrea Dal Corso^{1,2}

¹International School for Advanced Studies (SISSA),
Via Bonomea 265, 34136 Trieste (Italy).

²CNR-IOM,
Via Bonomea 265, 34136 Trieste (Italy).

E-mail: cmalica@sissa.it

Abstract. We calculate the temperature-dependent elastic constants of palladium, platinum, copper and gold within the quasi-harmonic approximation using a first-principles approach and evaluating numerically the second derivatives of the Helmholtz free-energy with respect to strain at the minimum of the free-energy itself. We find an overall good agreement with the experimental data although the anomalies of palladium and platinum reported at room temperature are not reproduced. The contribution of electronic excitations is also investigated: we find that it is non-negligible for the C_{44} elastic constants of palladium and platinum while it is irrelevant in the other cases. Its effect is not sufficient to explain the details of the anomalies found by experiments, not even when, in the case of platinum, we take into account the electron-phonon interaction. Lastly, the effect of the exchange and correlation functional is addressed and it is found that it is important at $T = 0$ K, while all functionals give similar temperature dependencies.

1. Introduction

The vibrational and thermodynamic properties of transition and noble metals and of their alloys are key ingredients to understand many industrial and technological processes. [1, 2, 3] Moreover, the comprehension of these properties for elemental metals is a fundamental prerequisite for the rational design of materials. In addition to the extensive experimental investigations [4], the prediction of thermodynamic properties via density functional theory (DFT) [5, 6] has been among the primary goals of first-principles studies for many years (see for instance Refs. [7, 8] and references therein).

In this context, the `thermo_pw` [9] code has been designed to compute efficiently, among other things, the thermodynamic properties of solids. Previous applications include the phonon dispersions, the thermal expansions, and the heat capacities of the hexagonal close packed (hcp) metals rhenium, technetium, [10] ruthenium, and osmium [11] and the anharmonic contributions to the mean square atomic displacements within the quasi-harmonic approximation (QHA) of silicon, ruthenium, magnesium, and cadmium [12].

Elastic constants (ECs) are other crucial quantities for crystal thermodynamics: they determine the crystal stability, thermal stresses, and sound velocities. For several decades DFT has provided ECs of solids, often within 10% from the experiment. However calculations have been usually limited to $T = 0$ K since the introduction of quantum and temperature effects requires a significant computational effort. As a result, there are now numerous theoretical ECs data at $T = 0$ K [13, 14, 15], but much less at finite temperatures. Some calculations do exist, but many of them are limited to the quasi-static approximation (QSA) where the temperature dependent elastic constants (TDECs) are calculated as second derivatives of the total energy with respect to strain (as at $T = 0$ K) at the minimum of the Helmholtz free-energy so accounting only for the effect of thermal expansion on the ECs. Only in a few papers the complete QHA method was applied (see, for example, Refs. [16, 17]). Other calculations make use of the *ab-initio* molecular dynamics method that, however, focus mainly on the high temperature behavior where quantum effects can be neglected [18].

The `thermo_pw` code can compute the ECs at $T = 0$ K (see for instance [19] and references therein) and, recently, the implementation was extended to the calculation of the quasi-harmonic TDECs as second derivatives of the Helmholtz free-energy with respect to strain [20]. So far, applications include the TDECs of silicon, aluminum, silver, [20] and boron arsenide [21].

In this work, we apply this approach to other four paradigmatic face-centered cubic (fcc) transition and noble metals: palladium, platinum, copper, and

gold. The first two elements, palladium and platinum, present anomalies in the experimental TDECs that are not well understood, while the latter two are more regular. Already after the early measurements on palladium and platinum some models were put forward to explain the anomalous temperature dependence of their elastic constants [22, 23, 24, 25] and recently a computational DFT study has supported this interpretation [26]. These studies pointed out that the TDECs of palladium and platinum are anomalous due to the partially filled d bands whose electrons contribute substantially to the free-energy. This theoretical study focused on the electronic contribution to the TDECs while the phonon contribution was accounted for within the QSA. Another theoretical study within the QSA, instead, finds a conventional temperature dependence for all the ECs of palladium, even considering the electronic thermal excitations [27].

Here we extend the previous QHA implementation in order to include the effects of the electronic excitations on the TDECs and compare the electronic and vibrational contributions. We find that the electronic contribution, although smaller than the vibrational one, is relevant for the temperature dependence of the C_{44} ECs of palladium and platinum, where it improves the comparison with experiment, but it is not sufficient to reproduce in detail the anomalies. On the contrary, in copper and gold, whose d shells are completely filled, the electronic contribution to the TDECs is negligible.

Focusing on platinum we investigate also another possible source of anomalous behavior. Actually electronic excitations might change the phonon frequencies especially at high temperatures, so we calculate the effect of this change on the TDECs. We find no substantial contribution, not even at the highest studied temperature of $T = 1000$ K.

Finally, since so far the effect of the exchange and correlation functionals on the TDECs has not been addressed in detail, we do also a systematic comparison between the local density approximation (LDA) and the generalized gradient approximation (GGA), taking the available experimental data as a reference. We find that all functionals give similar softenings of the ECs with temperature, hence the functional that matches better the experimental ECs at $T = 0$ K turns out to be also the one that matches better the TDECs.

2. Theory

The QHA approach to the TDECs is detailed in the recent works [20, 21]: in this Section we limit ourselves to a summary of the most important formulas in order to make the paper self-contained and discuss how we have introduced the electronic excitations in the

calculation.

The isothermal elastic constants are obtained from the derivatives of the Helmholtz free-energy F with respect to strain ϵ :

$$\tilde{C}_{ijkl}^T = \frac{1}{\Omega} \left(\frac{\partial^2 F}{\partial \epsilon_{ij} \partial \epsilon_{kl}} \right)_{\epsilon=0}, \quad (1)$$

where Ω is the unit cell volume.

From the previous Equation the free-energy F contains a term quadratic in the strains:

$$F = \frac{\Omega}{2} \sum_{ijkl} \epsilon_{ij} \tilde{C}_{ijkl}^T \epsilon_{kl}. \quad (2)$$

In cubic solids there are three independent ECs, C_{1111} , C_{1122} and C_{2323} which, for symmetry reasons [28] are usually written in Voigt's notation as C_{11} , C_{12} and C_{44} , respectively. We compute them using the deformations:

$$\epsilon_A = \begin{pmatrix} \epsilon_1 & 0 & 0 \\ 0 & \epsilon_1 & 0 \\ 0 & 0 & \epsilon_1 \end{pmatrix}, \quad \epsilon_E = \begin{pmatrix} 0 & 0 & 0 \\ 0 & 0 & 0 \\ 0 & 0 & \epsilon_3 \end{pmatrix}, \quad (3)$$

$$\epsilon_F = \begin{pmatrix} 0 & \epsilon_4 & \epsilon_4 \\ \epsilon_4 & 0 & \epsilon_4 \\ \epsilon_4 & \epsilon_4 & 0 \end{pmatrix}.$$

The strain ϵ_A does not change the shape of the cubic cell, while ϵ_E transforms it into a tetragonal cell and ϵ_F into a rhombohedral cell. None of them conserves the volume of the cell.

As we are interested in the ECs obtained from the stress-strain relationship (C_{ijkl}^T without *tilde*), when the system is under a pressure p , we correct the \tilde{C}_{ijkl}^T [29]:

$$C_{ijkl}^T = \tilde{C}_{ijkl}^T + \frac{1}{2} p (2\delta_{ij}\delta_{kl} - \delta_{il}\delta_{jk} - \delta_{ik}\delta_{jl}). \quad (4)$$

The Helmholtz free-energy of Eq. 2 is obtained as the sum of the DFT total energy U , the vibrational and the electronic free energies $F = U + F_{vib} + F_{el}$. The vibrational free-energy is given by:

$$F_{vib}(\epsilon, T) = \frac{1}{2N} \sum_{\mathbf{q}\eta} \hbar\omega_\eta(\mathbf{q}, \epsilon) + \frac{k_B T}{N} \sum_{\mathbf{q}\eta} \ln \left[1 - \exp \left(-\frac{\hbar\omega_\eta(\mathbf{q}, \epsilon)}{k_B T} \right) \right] \quad (5)$$

where N is the number of cells in the crystal, $\omega_\eta(\mathbf{q}, \epsilon)$ is the phonon angular frequency of the mode η with wave-vector \mathbf{q} computed in the system with a strain ϵ . The $\omega_\eta(\mathbf{q}, \epsilon)$ are computed by density functional perturbation theory (DFPT) [30] on a coarse \mathbf{q} -point mesh and Fourier interpolated on a thicker mesh to perform the Brillouin zone summation.

In order to account for the thermal electronic excitations [31], one could use the Mermin's finite temperature extension to DFT [32]. In this method, one minimizes the free-energy $U - TS_{el}$ where both U and the electronic entropy S_{el} are calculated using the Fermi-Dirac occupations at a given fixed temperature T . The method is accurate but needs a self-consistent calculation for each temperature. In order to evaluate the electronic free-energy for many temperatures we compute the total energy U with a Methfessel-Paxton smearing [33] and a broadening sufficiently small to get the zero broadening value of U and then use the $T = 0$ K DFT energy bands to calculate the contribution of electronic thermal excitations to the free-energy: F_{el} . We take $F_{el} = U_{el} - TS_{el}$ where U_{el} is the electronic excitations energy:

$$U_{el} = \int_{-\infty}^{+\infty} EN(E)f dE - \int_{-\infty}^{E_F} EN(E)dE, \quad (6)$$

while S_{el} is the electronic excitations entropy:

$$S_{el} = -k_B \int_{-\infty}^{+\infty} [f \ln f + (1-f) \ln(1-f)] N(E) dE \quad (7)$$

In Eqs. 6 and 7 $f(E, \mu, T)$ are the Fermi-Dirac occupations (depending on E , the temperature T , and the chemical potential μ), $N(E)$ is the electronic density of states and E_F is the Fermi energy. The μ is calculated at each temperature imposing that the number of electrons per unit cell N_{el} is determined by $N_{el} = \int_{-\infty}^{+\infty} N(E)f(E, T, \mu) dE$.

The QHA calculation of the ECs, Eq. 1, is performed on a grid of reference geometries by varying the lattice constant a_0 . Phonon dispersions and electronic bands are computed on the same grid in order to evaluate the total Helmholtz free-energy as a function of the volume. Then, at each temperature T , the ECs are interpolated and evaluated at the $a(T)$ which minimizes the free-energy. The calculation requires phonon dispersions and electronic band structures in all the strained configurations for all the reference geometries.

In order to compare our results with ultrasonic experimental data we compute also the adiabatic ECs given by:

$$C_{ijkl}^S = C_{ijkl}^T + \frac{T\Omega b_{ij} b_{kl}}{C_V}, \quad (8)$$

where b_{ij} are the thermal stresses:

$$b_{ij} = - \sum_{kl} C_{ijkl}^T \alpha_{kl}, \quad (9)$$

and α_{kl} is the thermal expansion tensor. C_V is the isochoric heat capacity defined, for example, in Ref. [21] and Ω is the unit cell volume at the temperature T .

The DFPT phonon calculation can be also performed at finite temperature T_{FD} by using

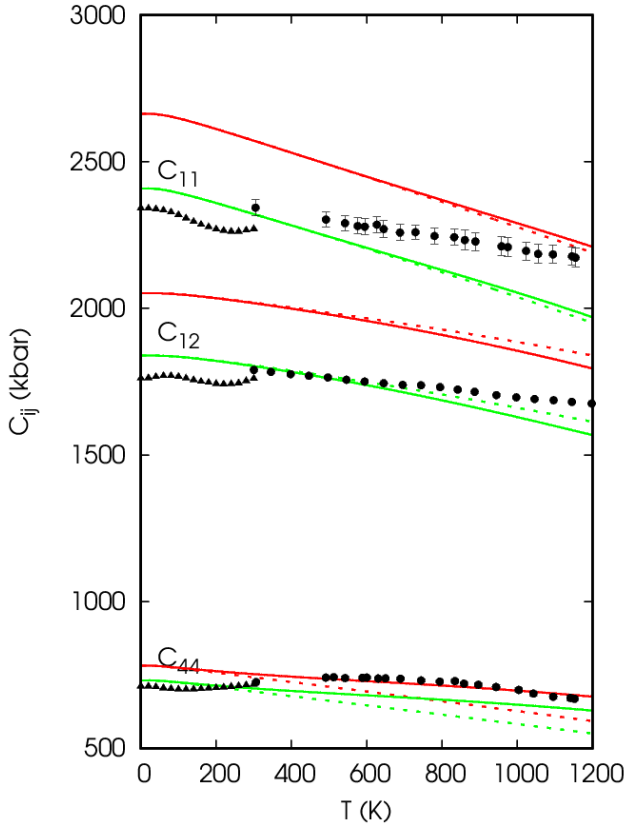


Figure 1. Quasi-harmonic adiabatic elastic constants of palladium. LDA (red curves) is compared with PBEsol (green curves). The results obtained with the total free-energy (continuous lines) are compared with those in which the contribution of electronic excitations is neglected (dashed lines). Experimental data are taken from Rayne [22] (black triangles) and [24] (black circles).

Fermi-Dirac occupations [34] with a broadening corresponding to the given temperature. Hence, the angular frequency $\omega_\eta(\mathbf{q}, \epsilon)$ of Eq. 5 are replaced with the temperature dependent $\omega_\eta(\mathbf{q}, \epsilon, T_{FD})$, giving a correction to the Helmholtz free-energy. In this case the electronic excitations contribution is already included in the DFT total energy U , via the Mermin’s functional, and it is not necessary to add it separately. We use this approach in platinum at enough large temperatures in order to clearly identify the effect, in particular at the temperatures $T_{FD} = 800$ K and $T_{FD} = 1000$ K and compare with the former method.

3. Computational parameters

The calculations presented in this work were carried out using DFT as implemented in the Quantum ESPRESSO package [44] [45]. For the calculations of ECs at $T = 0$ K and for all materials, the exchange and correlation functional was approximated

by the local density approximation (LDA) [46], the generalized gradient approximation (GGA) of Perdew, Burke and Ernzerhof (PBE) [47] and its modification for densely packed solids (GGA-PBEsol) [48]. For the TDECs we use LDA and GGA-PBEsol for all metals and for copper we also use the GGA-PBE functional (which, in this case, gives the best agreement with the experimental $T=0$ K ECs). We employ the projector augmented wave (PAW) method and a plane waves basis set with pseudopotentials [49] from `pslibrary` [50]. The pseudopotentials are reported in the note ‡. The cutoff for the wave functions (charge density) was 60 Ry (400 Ry) for palladium, 45 Ry (300 Ry) for platinum, 60 Ry (1200 Ry) for copper and 60 Ry (400 Ry) for gold. The presence of the Fermi surface has been dealt with by a smearing approach [33] with a smearing parameter $\sigma = 0.005$ Ry for palladium and platinum and $\sigma = 0.02$ Ry for copper and gold. The \mathbf{k} -point mesh was $40 \times 40 \times 40$ (except for PBEsol gold, for which a mesh $48 \times 48 \times 48$ has been used). Density functional perturbation theory (DFPT) [30] [51] was used to calculate the dynamical matrices on a $8 \times 8 \times 8$ \mathbf{q} -point mesh for palladium and platinum (corresponding to 29 special \mathbf{q} -points for configurations strained with ϵ_A , 59 \mathbf{q} -points for ϵ_E and 65 for ϵ_F , see Ref. [20] for the definitions of the strains) and $4 \times 4 \times 4$ \mathbf{q} -point mesh for copper and gold (corresponding to 8 \mathbf{q} -points for configurations strained with ϵ_A and 13 \mathbf{q} -points for those strained with ϵ_E and ϵ_F). For palladium and platinum a thicker \mathbf{q} -points mesh was necessary due to the presence of Kohn anomalies [8]. For all materials the dynamical matrices have been Fourier interpolated on a $200 \times 200 \times 200$ \mathbf{q} -point mesh to evaluate the vibrational free-energy. The calculation of the TDECs is done by `thermo_pw` as described in Ref. [20]. The grid of reference geometries was centered at the minimum of the total energy as reported in Table 1 except for the LDA study of platinum that was centered at $a_0 = 3.916$ Å. We used 7 reference geometries separated by $\Delta a = 0.07$ a.u. for all metals except for platinum where we used $\Delta a = 0.0233$ a.u. for LDA and $\Delta a = 0.03$ a.u. for PBEsol due to the presence of unstable strained configurations with imaginary phonon frequencies at too large lattice constants. We used 6 strained configurations for each type of strain with a strain interval $\delta\epsilon = 0.005$. In total we computed the phonon dispersions on 126 geometries for each material and functional in addition to those

‡ For palladium we used `Pd.pz-n-kjpaw-ps1.1.0.0.UPF` and `Pd.pbesol-n-kjpaw-ps1.1.0.0.UPF`. For platinum `Pt.pz-n-kjpaw-ps1.1.0.0.UPF` and `Pt.pbesol-n-kjpaw-ps1.1.0.0.UPF`. For copper `Cu.pz-dn-kjpaw-ps1.1.0.0.UPF`, `Cu.pbe-dn-kjpaw-ps1.1.0.0.UPF` and `Cu.pbesol-dn-kjpaw-ps1.1.0.0.UPF`. For gold we used `Au.pz-dn-kjpaw-ps1.0.3.0.UPF` and `Au.pbesol-dn-kjpaw-ps1.0.3.0.UPF`.

Table 1. ECs at $T = 0$ K computed with LDA, PBEsol and PBE exchange and correlation functionals compared with previous theoretical works and experimental data. The equilibrium lattice constants (a_0) are in Å while the ECs and the bulk moduli B are in kbar. The bulk modulus is $B = \frac{1}{3}(C_{11} + 2C_{12})$.

	a_0	C_{11}	C_{12}	C_{44}	B
Palladium					
LDA	3.85	2696	2071	788	2279
PBEsol	3.88	2445	1861	740	2056
PBE	3.95	2010	1532	606	1690
LDA ^a	3.90	2743	1463	716	1890
GGA ^b	3.94	2548	1358	587	1755
Expt. ^c	3.8896(2)	2341(27)	1761(27)	712(3)	1954
Platinum					
LDA	3.90	3800	2759	802	3106
PBEsol	3.92	3553	2581	764	2905
PBE	3.98	3039	2234	615	2502
LDA ^d	3.91	3645	2665	736	2992
PBEsol ^e	3.91	3595	2456	858	2836
GGA ^d	3.99	3063	2133	730	2443
Expt. ^f	3.92268(4)	3487(130)	2458(130)	734(20)	2801(9)
Copper					
LDA	3.52	2349	1666	998	1894
PBEsol	3.56	2100	1480	938	1687
PBE	3.63	1775	1238	793	1417
LDA ^g	3.64	1678	1135	745	1316
GGA ^h	3.63	1745	1253	752	1417
GGA ⁱ	3.63	1800	1200	840	1400
Expt. ^l	3.596	1762.0	1249.4	817.7	1420.3
Gold					
LDA	4.05	2120	1873	373	1955
PBEsol	4.10	1926	1651	366	2614
PBE	4.16	1544	1327	268	1389
GGA ^g	4.07	2021	1742	379	1835
PBE ^m	4.19	1478	1435	387	1449
Expt. ⁿ	4.062	2016.3	1696.7	454.4	1803.2

^a Ref. [27], ^b Ref. [35]

^c Ref. [22] (room temperature a_0 , $T = 0$ K extrapolation of ECs),

^d Ref. [36], ^e Ref. [15] (all electrons),

^f Reference [37] (room temperature results, most recent work)

^g Reference [13], ^h Reference [38], ⁱ Reference [39]

^l Ref. [40] for a_0 and Ref. [41] for the ECs ($T = 0$ K extrapolation),

^m Ref. [42], ⁿ Ref. [40] for a_0 and Ref. [43] for the ECs ($T = 0$ K extrapolation)

computed on the reference configurations required to compute $a(T)$ and the thermal expansion. For the electronic calculation we computed the bands in all the reference configurations (to include the effect on $a(T)$) and in all the strained ones (to include it in the TDECs). The \mathbf{k} -point mesh for the electronic DOS calculations was $48 \times 48 \times 48$. We use a Gaussian smearing with a smearing parameter of 0.01 Ry. The inclusion of the electronic finite temperature effect in the thermodynamic quantities and in the TDECs is documented in the `thermo_pw` user's guide. In order to fit the free-energy as a function of the strain we

used a polynomial of degree two because, although the use of a fourth-degree polynomial could introduce some differences, it requires higher cutoffs to converge the $T = 0$ K ECs. To interpolate the ECs computed at the different reference configurations and calculate them at the temperature dependent geometry we use a fourth-degree polynomial. More informations about the convergence tests are reported in the supplementary material.

The DFPT finite-temperature approach was applied to evaluate the ECs of platinum at the temperatures $T_{FD} = 800$ K (with a Fermi-Dirac

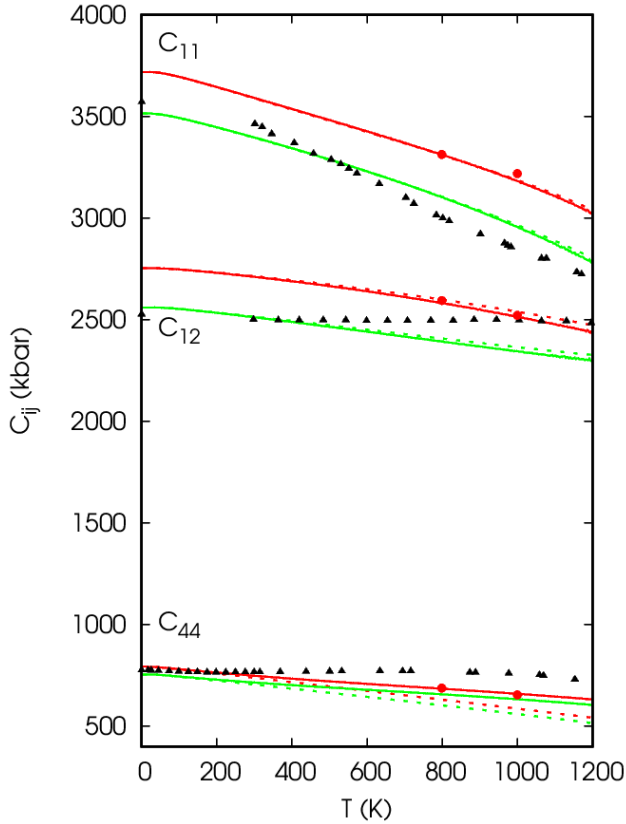


Figure 2. Quasi-harmonic adiabatic elastic constants of platinum. LDA (red curves) is compared with PBEsol (green curves). The results obtained with the total free-energy (continuous line) are compared with those in which the contribution of electronic excitations is neglected (dashed lines). The red circles at 800K and 1000K are computed within the LDA by using the Fermi-Dirac occupations. Experimental data are taken from Collard and McLellan [25] (black triangles).

smearing $\sigma_{FD} \approx 0.005$ Ry) and $T_{FD} = 1000$ K ($\sigma_{FD} \approx 0.0063$ Ry). For this purpose the TDECs calculation was set in a single reference geometry with the lattice constant at the considered temperature: 7.429 a.u. for 800 K and 7.446 a.u. for 1000 K.

4. Applications

In Table 1, we report the zero temperature lattice constants, elastic constants, and bulk moduli of the four metals calculated with different exchange and correlation functionals. We compare them with experiments and previous theoretical works. As usually found, PBE and PBEsol give slightly larger lattice parameters than LDA and smaller $T = 0$ K ECs. PBEsol reproduces the experimental ECs of palladium and platinum better than LDA and PBE with errors smaller than $\approx 5\%$ for all the ECs, compared to LDA errors in the range 10 – 18% in palladium and from

$\approx 9\%$ (C_{11} and C_{44}) to $\approx 12\%$ (C_{12}) in platinum. PBE has differences till to $\approx 15 - 16\%$ for both materials.

On the other hand, the experimental ECs of copper are well reproduced by PBE with errors equal or smaller than 3%, compared with errors larger than 15% for the other functionals. The LDA and PBEsol have almost the same accuracy in reproducing the $T = 0$ K C_{11} and C_{44} of gold (with errors of $\approx 5\%$ and $\approx 18\%$, respectively), while for C_{12} PBEsol has an error of $\approx 3\%$ and LDA an error of $\approx 10\%$, PBE has errors of $\approx 22\%$ in C_{11} and C_{12} and $\approx 40\%$ in C_{44} .

The differences found for the LDA ECs of palladium with respect to those of Ref. [27] are $\approx 2\%$ for C_{11} , $\approx 29\%$ for C_{12} and $\approx 10\%$ for C_{44} . For platinum, comparing our LDA ECs with the calculations of Ref. [36] we found differences of $\approx 4\%$ for C_{11} , $\approx 3\%$ for C_{12} and $\approx 8\%$ for C_{44} ; while the comparison of our PBEsol ECs with the corresponding PBEsol all-electrons calculation of Ref. [15] gives differences of $\approx 1\%$ for C_{11} , $\approx 5\%$ for C_{12} and C_{44} . The differences found for the LDA-ECs of copper with respect to those of Ref. [13] are $\approx 28\%$ for all ECs, while the differences between our PBE ECs with the other GGA ECs of Refs. [38, 39] are smaller than $\approx 3\%$ for C_{11} and C_{12} and $\approx 5 - 6\%$ for C_{44} . Our PBEsol ECs of gold are close to the GGA estimates of Ref. [13] with differences of $\approx 5\%$ for C_{11} and C_{12} and $\approx 3\%$ for C_{44} . For reference, in palladium, platinum, and gold we report GGA ECs found in literature. As expected, they are smaller than our LDA and PBEsol ECs. They shows some differences with our PBE estimates, which are, however, very close to the PBE ECs reported in the Materials Project database and computed with the PAW method.

In Figs. 1, 2, 3, 4 we report the TDECs of the four metals. For each plot we follow the same color-line convention: Red indicates LDA estimates, green PBEsol and blue, present only in copper, PBE. The continuous lines are computed by considering all contributions in the Helmholtz free-energy, while the dashed lines have been obtained neglecting the contribution of the electron thermal excitations. Black points are the experimental data.

The TDECs of palladium are shown in Fig. 1. Two experimental data-set are reported. The variation of the experimental ECs of Ref. [22] in the range 0 – 300 K is 3% for C_{11} , about 0% for C_{12} and -1% for C_{44} with respect to the 0 K ECs. The corresponding LDA (PBEsol) variations in the same range of temperature are 3.7% (4.5%) for C_{11} , 2% (2%) for C_{12} and 3.8% (3.8%) for C_{44} . In the range $T = 300 - 1200$ K the variations in the data of Ref. [24] are 7.3% for C_{11} , 6.4% for C_{12} and 7.8% for C_{44} , while the corresponding theoretical softenings are 15% for C_{11} , 13% for C_{12} , 11% for C_{44} for both functionals.

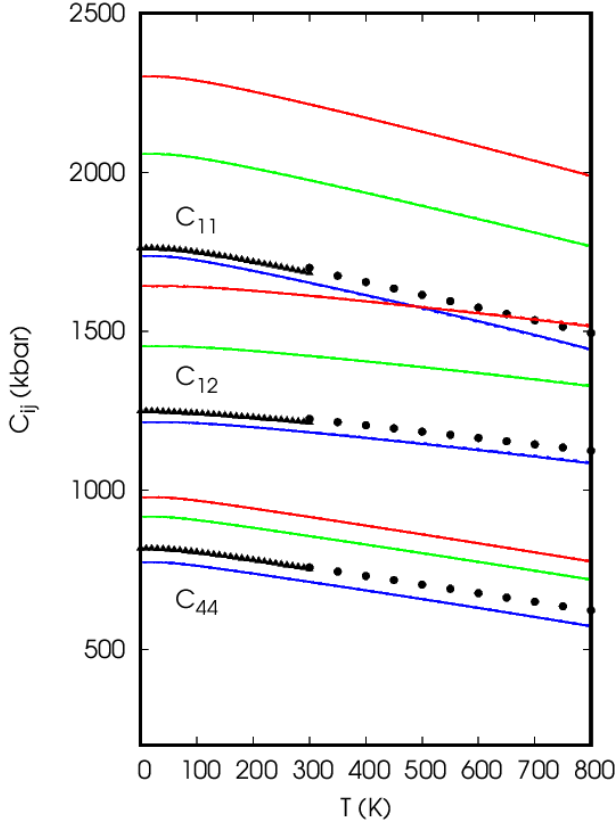


Figure 3. Quasi-harmonic adiabatic elastic constants of copper. LDA (red curves), PBEsol (green curves) and PBE (blue) are compared. The results obtained with the total free-energy (continuous line) overlaps those in which the contribution of electronic excitation is neglected (dashed lines). Experimental data are taken from Overton and Gaffney [41] (black triangles) and Chang and Himmel [52] (black circles).

Hence, both functionals give a similar temperature dependence. At room temperature the details of the experimental anomalies are not reproduced and above room temperature the theoretical softening is larger than the experimental one. The electronic effect is very small in C_{11} and C_{12} but leads to appreciable modifications of C_{44} which becomes closer to the experiment. As expected, the electronic contribution increases with temperature and influences the softening of C_{44} that without the electronic effect would be 20% in the range 300 – 1200 K.

The TDECs of platinum are reported in Fig. 2. From $T = 0$ K to $T = 1200$ K the experimental ECs decrease of about 24% for C_{11} , about 2% for C_{12} and about 6% for C_{44} . The corresponding theoretical softening for LDA (PBEsol) are 18% (20%) for C_{11} , 11% (10%) for C_{12} and 19% (19%) for C_{44} . Hence, the variation of C_{11} is well reproduced while the other two ECs’ softenings are overestimated. As found for palladium, the electronic contribution is important and

improves the comparison with the experiment only for the C_{44} EC: without the electronic effect the softening would be $\approx 30\%$. However, it can not describe the anomalies. In order to further investigate the trend of the ECs of platinum we also considered the effect of the electronic excitation on the phonon frequencies for the temperatures $T = 800$ K and $T = 1000$ K with the method explained in the previous section (results are reported in red circles in the plot, only for the LDA case). The red points are exactly over our curves (apart for a slight deviation in the C_{11} at 1000 K). This fact points out that the electron-phonon interactions that modify the phonon frequencies has negligible consequences on the TDECs. We observe that our estimate of the electronic contribution is smaller than the one of Ref. [26] even for the C_{44} . In our calculation the largest contribution is the vibrational one which always decreases the ECs as the temperature increases. In Ref. [26] the vibrational contribution is described within a quasi-static framework which leads to an underestimation of the ECs’ softening. Our results are qualitatively closer to those of Ref. [27] that finds a conventional temperature dependence for the C_{44} .

The results of copper are shown in Fig. 3. Since the two different experimental set of data are smoothly connected we report the whole softening in the range of temperature $T = 0 - 800$ K: 15% for C_{11} , 10% for C_{12} and 24% for C_{44} . The corresponding theoretical softening for LDA (PBEsol, PBE) are 13.5% (14%, 17%) for C_{11} , 7.6% (8.5%, 10.5%) for C_{12} and 21% (21%, 26%) for C_{44} . The temperature dependence is almost the same for LDA and PBEsol, slightly larger for PBE. The estimated softenings agree very well with the experiment. PBE results are the closest to the experiment, reflecting the trend of the $T = 0$ K ECs shown in Table 1. The electronic thermal excitations do not give any observable contribution in the whole range of temperature.

The TDECs of gold are shown in Fig. 4. As for copper we consider the two experiments together: In the range of temperature from $T = 0$ K to $T = 800$ K the softenings are 13% for C_{11} , 11% for C_{12} and 22% for C_{44} . The corresponding softening for LDA (PBEsol) are 18% (22%) for C_{11} , 17% (20%) for C_{12} and 24% (29%) for C_{44} . The PBEsol softening is slightly larger than the LDA one and both functionals overestimate the experimental softening in particular for C_{11} and C_{12} with differences that increase from room temperature onward. As in copper, the electronic thermal excitations do not give any observable contribution.

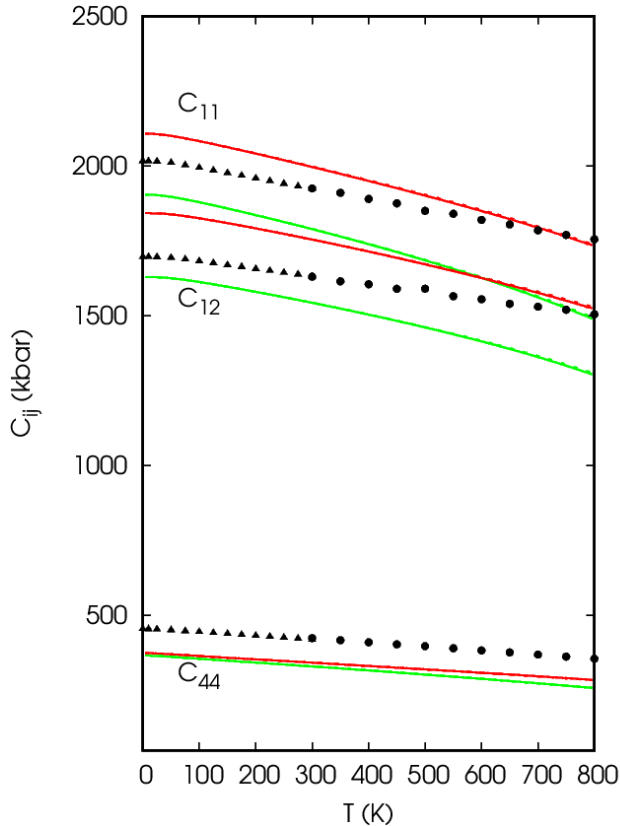


Figure 4. Quasi-harmonic adiabatic elastic constants of gold. LDA (red curves) and PBEsol (green curves) are compared. The results obtained with the total free-energy (continuous lines) overlaps with those in which the contribution of electronic excitation is neglected (dashed lines). Experimental data are taken from Neighbours and Alers [43] (black triangles) and Chang and Himmel [52] (black circles).

5. Conclusions

In this paper we investigated the TDECs of palladium, platinum, copper, and gold by means of the QHA. LDA and GGA give almost the same softenings but differ in the zero temperature values. This work shows that PBEsol is the best choice for palladium, platinum, and gold. PBE is the best for copper. Moreover, we addressed the role of the thermal electronic excitations and found a negligible effect on the TDECs of copper and gold, and an improvement in the agreement with the experimental C_{44} of palladium and platinum. Even though the computed softenings of all ECs is in reasonable agreement with the experimental ones, we could not reproduce the precise behavior of the anomalies in platinum and palladium. In platinum, we further investigated the effects of the change of the phonon frequencies induced by the finite temperature thermal electronic excitations, finding that it is small, even at the highest studied temperature $T = 1000$ K.

At the current stage the discrepancy between theory and experiment in palladium and platinum is not solved and might require either a more sophisticated functional than LDA or GGA or a method that includes the anharmonic effects beyond the QHA approximation [53]. Since the experimental data are quite old, also a novel measurement of the TDECs could be useful.

Acknowledgments

Computational facilities have been provided by SISSA through its Linux Cluster and ITCS and by CINECA through the SISSA-CINECA 2019-2021 Agreement.

References

- [1] N. Saunders A.P. Miodownik. *CALPHAD*. Pergamon, 1998.
- [2] H. L. Lukas, S. G. Fries, and B. Sundman. *Computational thermodynamics*. Cambridge University Press, 2007.
- [3] S. Curtarolo, W. Setyawan, G.L.W. Hart, M. Jahnatek, R. V. Chepulskii, R. H. Taylor, S. Wang, J. Xue, K. Yang, O. Levy, M. J. Mehl, H. T. Stokes, D. O. Demchenko, and D. Morgan. *Computational Materials Science*, 58:218–226, 2012.
- [4] Y. S. Touloukian, R. K. Kirby, R. E. Taylor, and P. D. Desai. *Thermal expansion: Metallic elements and alloys*. IFI/Plenum, 1975.
- [5] P. Hohenberg and W. Kohn. *Phys. Rev.*, 136:B864–B871, 1964.
- [6] W. Kohn and L. J. Sham. *Phys. Rev.*, 140:A1133–A1138, 1965.
- [7] B. Grabowski, T. Hickel, and J. Neugebauer. *Phys. Rev. B*, 76:024309, Jul 2007.
- [8] A. Dal Corso. *J. Phys.: Condens. Matter*, 25(14):145401, mar 2013.
- [9] A. Dal Corso. <https://dalcorso.github.io/thermo-pw>, 2014.
- [10] M. Palumbo and A. Dal Corso. *Phys. Status Solidi B*, 254:1700101, 2017.
- [11] M. Palumbo and A. Dal Corso. *J. Phys.: Condens. Matter*, 29:395401, 2017.
- [12] C. Malica and A. Dal Corso. *Acta Cryst. Section A*, 75(4):624–632, Jul 2019.
- [13] H. Wang and M. Li. *Phys. Rev. B*, 79:224102, Jun 2009.
- [14] R. Golezorkhtabar, P. Pavone, J. Spitaler, P. Puschnig, and C. Draxl. *Comput. Phys. Commun.*, 184(8):1861–1873, 2013.
- [15] M. Jamal, S. Jalali Asadabadi, Iftikhar Ahmad, and H.A. Rahnamaye Aliabad. *Computational Materials Science*, 95:592–599, 2014.
- [16] B. B. Karki, R. M. Wentzcovitch, S. de Gironcoli, and S. Baroni. *Science*, 286(5445):1705–1707, 1999.
- [17] D. Dragoni, D. Ceresoli, and N. Marzari. *Phys. Rev. B*, 91:104105, Mar 2015.
- [18] P. Steneteg, O. Hellman, O. Y. Vekilova, N. Shulumba, F. Tasnádi, and I. A. Abrikosov. *Phys. Rev. B*, 87:094114, 2013.
- [19] A. Dal Corso. *Journal of Physics: Condensed Matter*, 28(7):075401, jan 2016.
- [20] C. Malica and A. Dal Corso. *J. Phys. Condens. Matter*, 32:315902, 2020.
- [21] C. Malica and A. Dal Corso. *J. Appl. Phys.*, 127:245103, 2020.
- [22] J. A. Rayne. *Phys. Rev.*, 118:1545, 1960.

- [23] C. Weinmann and S. Steinemann. *Solid State Comm.*, 15:281, 1974.
- [24] M. Yoshihara, R.B. McLellan, and F.R. Brotzen. *Acta Metallurgica*, 35(3):775–780, 1987.
- [25] S. M. Collard and R. B. McLellan. *Acta metall. mater.*, 40:699, 1992.
- [26] P. Keuter, D. Music, V. Schnabel, M. Stuer, and J. M Schneider. *J. Phys.: Condens. Matter*, 31:225402, 2019.
- [27] Z-L. Liu, J-H. Yang, L-C. Cai, F-Q. Jing, and D. Alfè. *Phys. Rev. B*, 83:144113, 2011.
- [28] J. F. Nye. *Physical properties of crystals*. Oxford science publications New York, 1985.
- [29] T. H. K. Barron and M. L. Klein. *Proc. Phys. Soc.*, 85:523, 1965.
- [30] S. Baroni, S. de Gironcoli, A. Dal Corso, and P. Giannozzi. *Rev. Mod. Phys.*, 73:515, 2001.
- [31] X. Zhang, B. Grabowski, F. Körmann, C. Freysoldt, and J. Neugebauer. *Phys. Rev. B*, 95:165126, 2017.
- [32] N. David Mermin. *Phys. Rev.*, 137:A1441–A1443, 1965.
- [33] M. Methfessel and A. T. Paxton. *Phys. Rev. B*, 40:3616–3621, 1989.
- [34] S. de Gironcoli. Lattice dynamics of metals from density-functional perturbation theory. *Phys. Rev. B*, 51:6773–6776, 1995.
- [35] T. Gao and J. R. Kitchin. *Catalysis Today*, 312:132–140, 2018.
- [36] V.I. Razumovskiy, E.I. Isaev, A.V. Ruban, and P.A. Korzhavyi. *Intermetallics*, 16(8):982–986, 2008.
- [37] S. Kamada, H. Fukui, A. Yoneda, H. Gomi, F. Maeda, S. Tsutsui, H. Uchiyama, N. Hirao, D. Ishikawa, and A. Q.R. Baron. *C. R. Geoscience*, 351:236, 2019.
- [38] L. Yue-Lin, G. Li-Jiang, and Jin S. 21(9):096102, 2012.
- [39] M. Jahnátek, J. Hafner, and M. Krajčí. *Phys. Rev. B*, 79:224103, 2009.
- [40] P. Haas, F. Tran, and P. Blaha. *Phys. Rev. B*, 79:085104, 2009.
- [41] W. C. Overton and John Gaffney. *Phys. Rev.*, 98:969, 1955.
- [42] G-X. Kong, X-J M., Q-J. Liu, Y. Li, and Z-T. L. *Physica B: Condensed Matter*, 533:58–62.
- [43] J. R. Neighbours and G. A. Alers. *Phys. Rev.*, 111:707–712, Aug 1958.
- [44] P. Giannozzi, S. Baroni, N. Bonini, M. Calandra, R. Car, C. Cavazzoni, D. Ceresoli, G. L. Chiarotti, M. Cococcioni, I. Dabo, et al. *J. Phys.: Condens. Matter*, 21:395502, 2009.
- [45] P. Giannozzi, O. Andreussi, T. Brumme, O. Bunau, M. Buongiorno Nardelli, M. Calandra, R. Car, C. Cavazzoni, D. Ceresoli, M. Cococcioni, et al. *J. Phys.: Condens. Matter*, 29:465901, 2017.
- [46] J. P. Perdew and A. Zunger. *Phys. Rev. B*, 23:5048–5079, 1981.
- [47] J. P. Perdew, K. Burke, and M. Ernzerhof. *Phys. Rev. Lett.*, 77:3865–3868, 1996.
- [48] J. P. Perdew, A. Ruzsinszky, G. I. Csonka, O. A. Vydrov, G. E. Scuseria, L. A. Constantin, X. Zhou, and K. Burke. *Phys. Rev. Lett.*, 100:136406, Apr 2008.
- [49] P. E. Blöchl. *Phys. Rev. B*, 50:17953, 1994.
- [50] A. Dal Corso. <https://github.com/dalcorso/pslibrary>, 2010.
- [51] A. Dal Corso. *Phys. Rev. B*, 81:075123, 2010.
- [52] Y. A. Chang and L. Himmel. *J. Appl. Phys.*, 37(9):3567–3572, 1966.
- [53] N. Shulumba, O. Hellman, L. Rogström, Z. Raza, F. Tasnádi, I. A. Abrikosov, and M. Odén. *Applied Physics Letters*, 107(23):231901, 2015.

Supplementary material for Quasi-harmonic thermoelasticity of palladium, platinum, copper, and gold from first principles.

1. Convergence tests

In this section we discuss some convergence tests of the zero-temperature elastic constants (ECs) with respect to the energy cutoffs, smearing parameters and \mathbf{k} -points meshes. The ECs are computed by fitting the energy-strain curves. We used 6 value of the strain: a reasonable compromise between accuracy and the need to reduce the number of phonon calculations. To fit them, a second-degree polynomial was selected that, in the previous literature, was found to be the best polynomial to give the ECs for a small set of points (Computer Physics Communications **184**, 1861 (2013) and Physical Review B **85** 064101 (2012)). A higher polynomial degree, like fourth, requires larger energy cutoffs to converge the ECs. We discuss below the choice of the polynomial and the interval $\Delta\epsilon$ between strained configurations. For the following tests we used $\Delta\epsilon = 0.005$ which was found to be a good choice for many materials (see, for example, Refs. [16-18] of the paper).

Table 1: Convergence test of zero-temperature ECs vs. energy cutoffs with unconverged smearing parameter ($\sigma = 0.02$ Ry) and \mathbf{k} -points grid ($16 \times 16 \times 16$) computed within LDA. The ECs and the bulk moduli B are in kbar. The bulk modulus is $B = \frac{1}{3}(C_{11} + 2C_{12})$.

ecut_wf (ecut_rho)	a_0	C_{11}	C_{12}	C_{44}	B
Palladium					
45(300)	7.275	2725	2071	874	2289
60(400)	7.274	2699	2062	864	2274
100(800)	7.274	2723	2069	868	2287
Platinum					
45(300)	7.373	3819	2740	891	3100
60(400)	7.373	3811	2748	892	3102
100(800)	7.372	3818	2743	892	3101
Copper					
45(1200)	6.651	2359	1651	1005	1887
60(1200)	6.651	2376	1656	1008	1896
60(1600)	6.651	2373	1660	1010	1898
100(2000)	6.651	2372	1668	1010	1903
Gold					
45(300)	7.663	2162	1846	428	1951
60(400)	7.662	2138	1860	426	1953
100(800)	7.662	2168	1842	427	1951

In Table 1 the ECs as well as the lattice parameters and the bulk moduli are reported for increasing cutoffs. We started with the cutoffs needed to converge the phonon frequencies (Ref. [8] of the paper). We ensure that C_{11} and C_{12} are converged within at least ≈ 20 kbar and a few kbar for the C_{44} . The chosen cutoffs are written in bold type. The tests in the tables are for the LDA functional but the final cutoffs were chosen also considering the tests with the other functionals.

With the converged cutoffs we test the smearing parameter and the \mathbf{k} -points grids for each material. These tests are reported in Fig. 1. The final set of ECs are those obtained with the parameters declared in the paper ($\sigma = 0.005$ Ry for palladium and platinum, $\sigma = 0.02$ Ry for copper and gold and $N_k = 40$ for all systems).

In order to further check the ECs we compute them as the derivatives of the stress with respect to the strain. For this purpose we compute directly the stress (by using the stress theorem as implemented in *QuantumESPRESSO* and explained in Physical Review B **32** 3780 (1985)) in four strained configurations around the equilibrium and then fit with respect to the strain with a second-degree polynomial and evaluate the analytic first derivative. The results are collected in Table 2. The ECs computed within the two methods are in good agreement with differences usually less than 1%, only in the C_{11} and C_{12} ECs of copper the differences are $\approx 2\%$ but the agreement is still satisfactory.

Table 2: Comparison between ECs computed from the second derivatives of the total energy and those computed from the first derivatives of the stress with respect to the strain. We used the converged parameters discussed in Table 1 and Fig. 1. The functional is LDA. The ECs and the bulk moduli B are in kbar. The bulk modulus is $B = \frac{1}{3}(C_{11} + 2C_{12})$.

Method	C_{11}	C_{12}	C_{44}	B
Palladium				
Energy	2696	2071	788	2279
Stress	2705	2070	782	2282
Platinum				
Energy	3800	2759	802	3106
Stress	3788	2754	790	3099
Copper				
Energy	2349	1666	998	1894
Stress	2293	1625	998	1848
Gold				
Energy	2120	1873	373	1955
Stress	2130	1849	374	1943

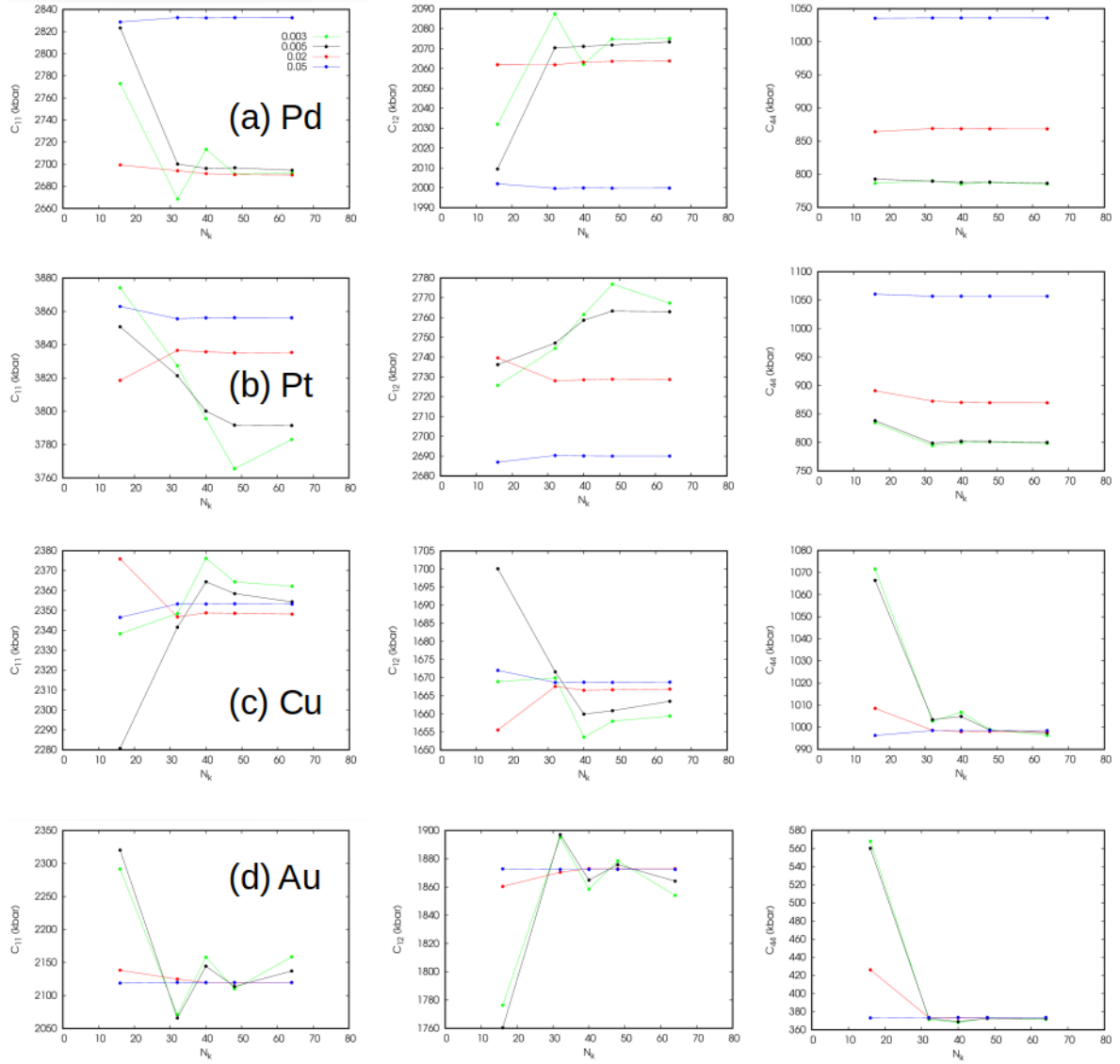


Figure 1: Tests of the zero temperature ECs vs. the smearing parameters and the k -points grid $N_k \times N_k \times N_k$ for each material. The color indicates the smearing parameter: $\sigma = 0.003$ Ry (green), $\sigma = 0.005$ Ry (black), $\sigma = 0.02$ Ry (red) and $\sigma = 0.05$ Ry (blue) The final set of parameters is $\sigma = 0.005$ Ry for palladium and platinum, $\sigma = 0.02$ Ry for copper and gold and $N_k = 40$ for all systems.

Finally, we check the parameters $\Delta\epsilon$ and the degree of the polynomial in Figure 2. The second degree polynomial (red) provides ECs equal or very similar ECs to those computed with the third degree polynomial (green): their values are the same in a reasonably large interval of $\Delta\epsilon$ around $\Delta\epsilon = 0.005$. While the fourth degree polynomial (blue) reaches the plateau for larger values of $\Delta\epsilon$. In any case the differences are usually very small, the largest differences between the second and fourth degree polynomial

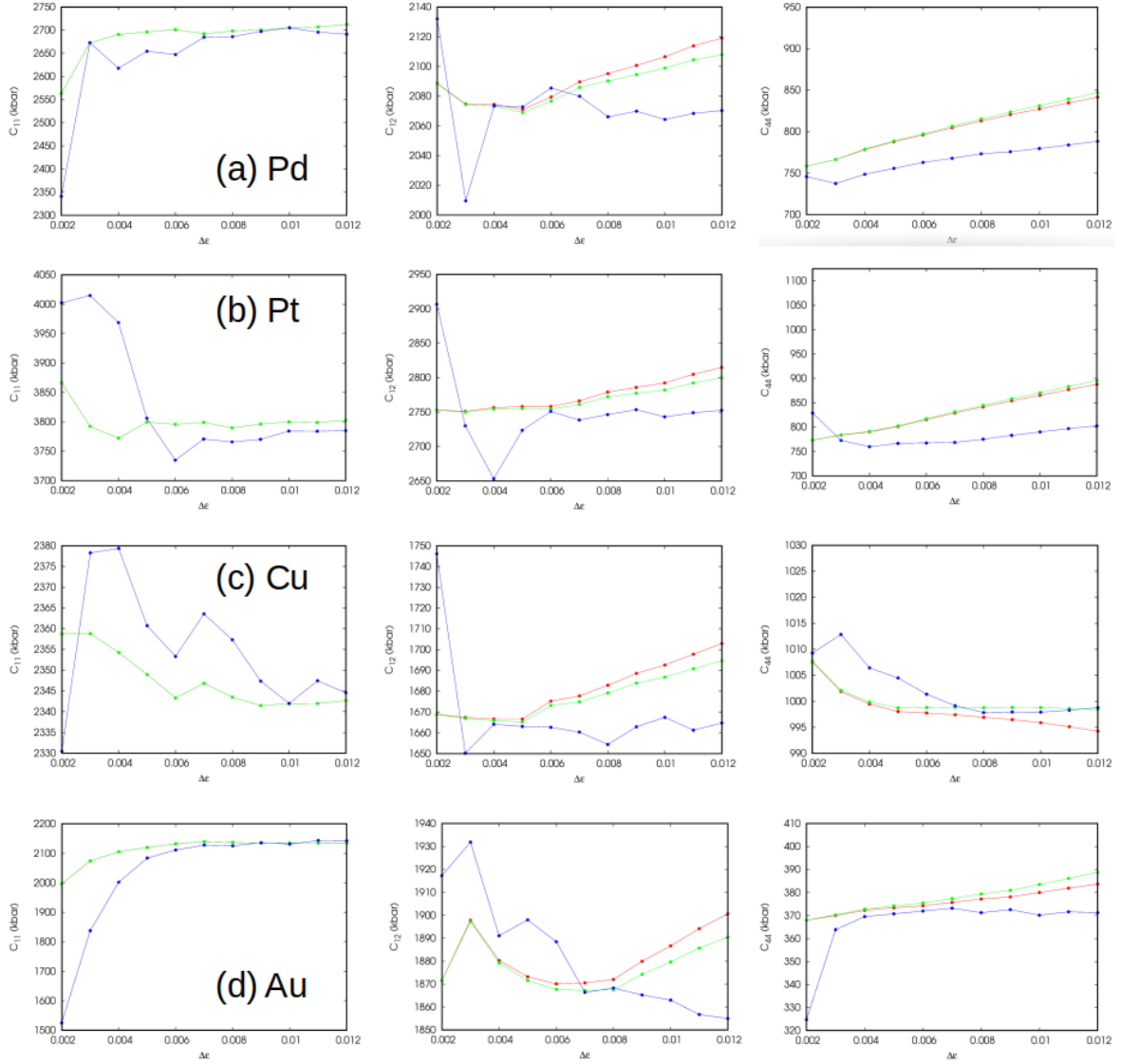


Figure 2: Tests as a function of the interval $\Delta\epsilon$ between two strained configuration for each EC of each material. The number of points is fixed at 6. The maximum applied strain can be obtained as $\epsilon_{max} = 2.5\Delta\epsilon$. Second degree (red), third degree (green) and fourth degree (blue) fitting polynomials are compared. The value chosen for the calculation is $\Delta\epsilon = 0.005$.

are found in the C_{44} ECs of palladium and platinum that are however of the order of 32 – 34 kbar with $\Delta\epsilon = 0.005$. This difference reduces if the ECs obtained from the fourth degree polynomial are computed with a larger cutoff. For example in palladium becomes 19 kbar with a cutoff equal to 110 Ry and 800 Ry for the wave functions and charge density, respectively.